

THE CRYSTAL STRUCTURE OF ARGENTOJAROSITE, $\text{AgFe}_3(\text{SO}_4)_2(\text{OH})_6$

LEE A. GROAT[§], JOHN L. JAMBOR AND BONNIE C. PEMBERTON

Department of Earth and Ocean Sciences, University of British Columbia, Vancouver, British Columbia V6T 1Z4, Canada

ABSTRACT

The crystal structure of natural argentojarosite, ideally $\text{AgFe}_3(\text{SO}_4)_2(\text{OH})_6$, a 7.3398(7), c 16.538(3) Å, V 771.4(2) Å³, space group $R\bar{3}m$, $Z = 3$, has been refined to an R_1 index of 2.8% based on 307 unique reflections measured using MoK α radiation on an automated four-circle diffractometer. The refined occupancy of the A site suggests that it is fully occupied by Ag, with Ag–O and Ag–OH bond distances of 2.963 and 2.721 Å, respectively, and an $\text{AgO}_6(\text{OH})_6$ icosahedral volume of 57.71 Å³. Whereas Ag^+ in argentojarosite is in 12-fold coordination, for which the ionic radius is projected to be 1.48–1.56 Å, the crystal-structure results suggest that the radius is 1.35–1.36 Å, closer to the value expected for nine-fold coordination. Consequently, the coordination sphere of Ag^+ in argentojarosite is perhaps best thought of as intermediate between six- and 12-coordination. Twelve-fold coordination of Ag is not known in any other mineral, and there is a strong possibility that the published bond-valence curves cannot be applied to this coordination of Ag.

Keywords: argentojarosite, crystal structure, jarosite group, alunite supergroup, silver.

SOMMAIRE

Nous avons affiné la structure cristalline de l'argentojarosite naturelle, dont la formule idéale est $\text{AgFe}_3(\text{SO}_4)_2(\text{OH})_6$, a 7.3398(7), c 16.538(3) Å, V 771.4(2) Å³, groupe spatial $R\bar{3}m$, $Z = 3$, jusqu'à un résidu R_1 de 2.8% sur une base de 307 réflexions uniques mesurées avec rayonnement MoK α et un diffractomètre automatisé à quatre cercles. Le taux d'occupation du site A indique qu'il est complètement rempli par les atomes Ag, avec des longueurs de liaison Ag–O et Ag–OH de 2.963 et 2.721 Å, respectivement, et un volume icosaédrique du polyèdre $\text{AgO}_6(\text{OH})_6$ de 57.71 Å³. Tandis que l' Ag^+ dans l'argentojarosite est sensé avoir une coordinence de 12, et par conséquent un rayon ionique entre 1.48 et 1.56 Å, nos résultats font penser que le rayon ionique est plutôt 1.35–1.36 Å, plus près de la valeur attendue pour une coordinence de neuf. Par conséquent, la sphère de coordinence de l' Ag^+ dans l'argentojarosite serait probablement intermédiaire entre six et douze. Une coordinence de 12 n'est pas établie pour l'argent dans d'autres minéraux, et il y a de fortes chances que les courbes publiées pour évaluer les valences de liaison ne s'appliquent pas à cette coordinence de l'argent.

(Traduit par la Rédaction)

Mots-clés: argentojarosite, structure cristalline, groupe de la jarosite, supergroupe de l'alunite, argent.

INTRODUCTION

Minerals of the alunite supergroup have been mined for centuries. For example, the alunite deposits at Tolfa, Italy, were the basis of alum manufacture there since the middle of the fifteenth century (Palache *et al.* 1951), and Fe-bearing members of the group are considered to have been among the principal sources of Ag smelted during pre-Roman or early Roman exploitation of the extensive gossans at Rio Tinto, Spain (Dutrizac *et al.* 1983). It was not until 1923, however, that argentojarosite, $\text{AgFe}_3(\text{SO}_4)_2(\text{OH})_6$, which is the sole Ag-dominant member of the group, was identified as a mineral species (Schempp 1923, Schaller 1923). Argentojarosite

has since been reported to occur at several localities (*e.g.*, Troxel & Morton 1962, Amorós *et al.* 1981, Pearl 1974, Nekrasov & Nikishova 1987), but the mineral is nevertheless relatively rare; the presence of argentojarosite to account for significant Ag values in gossan deposits is commonly assumed, but solid-solution substitution in other members of the group, particularly Pb-bearing members such as plumbojarosite and beudantite, more commonly accounts for the Ag (Dutrizac & Jambor 1985, 1987, Roca *et al.* 1999).

Interest in the minerals of the alunite supergroup, which includes phosphate- and arsenate-dominant members in addition to the sulfate-dominant members, has surged in recent years because of the prominence of

[§] E-mail address: lgroat@eos.ubc.ca

some of these minerals both as oxidation products of sulfide-bearing mine wastes and as precipitates from the resulting acidic effluents. Further environmental interest has also focused on the possibility of using these minerals as storage materials for toxic metals (Baron & Palmer 1996, Kolitsch & Pring 2001). Nevertheless, the jarosite-group compounds, those with the general formula $AG_3(TO_4)_2(OH)_6$, in which A is K, Na, NH_4 , H_3O , Ag, Tl, or $Pb_{0.5}$, G is Fe^{3+} , and T is SO_4 , are possibly more familiar to hydrometallurgists than to mineralogists. Over the past 30 years or so, precipitation of jarosite-group phases has been widely adopted, particularly in the zinc industry, as a means of controlling Fe, sulfate, alkalis, and other impurities in hydrometallurgical circuits. Under the conditions relevant to processing in zinc plants, Ag is selectively incorporated in the precipitates in preference to Na, NH_4 , or Pb (Dutrizac 1983, Dutrizac & Jambor 1985, 1987). Among the Ag–Na– NH_4 –Pb-bearing jarosite-group compounds, the crystal structure of the Pb member has been determined (Szymański 1985), and that of the Na member is in progress (Gasharova *et al.* 2000), but various aspects of the structural relationships are still puzzling (Dutrizac & Jambor 1987, Jambor 1999, Göttlicher & Gasharova 1999, Göttlicher *et al.* 2000, Kolitsch & Pring 2001). As part of a more extensive study of the crystal chemistry of the alunite supergroup, we report here on the crystal structure of argentojarosite.

X-RAY CRYSTALLOGRAPHY AND CRYSTAL-STRUCTURE DETERMINATION

Experimental

The sample used in this study is from the Tintic Standard mine at Dividend, central Utah (Canadian Museum of Nature Mineral Collection, no. 59664). The crystals occur as thin hexagonal plates, up to 100 μm across and 7 μm thick, that are optically uniaxial. A Philips XL30 scanning electron microscope equipped with a Princeton Gamma-Tech energy-dispersion X-ray spectrometer was used to obtain qualitative chemical data. The spectra show peaks corresponding to the expected elements

plus a minor amount of Al. An attempt to collect quantitative electron-microprobe data gave nonsensical results because of damage from the electron beam, probably either related to or exacerbated by the thinness of the sample. The crystal was mounted on a P4 Siemens automated four-circle diffractometer equipped with a molybdenum-target X-ray tube (operated at 55 kV, 35 mA) and a precisely oriented graphite crystal monochromator mounted with equatorial geometry. Thirty-four reflections with $11.10 < 2\theta < 39.23^\circ$ were centered using an automated search routine, and the correct unit-cell was selected from an array of real-space vectors corresponding to potential unit-cell axes. Least-squares refinement of these reflections produced the cell dimensions given in Table 1, together with the orientation matrix relating the crystal axes to the diffractometer axes. Intensity data were collected in the θ – 2θ scan mode, using 96 steps with a scan range from $[2\theta(\text{MoK}\alpha_1) - 1.2]^\circ$ to $[2\theta(\text{MoK}\alpha_2) + 1.2]^\circ$ and a scan rate that varied between 1.0 and 20.0°/min depending on the intensity of an initial one-second count at the center of the scan range. Backgrounds were measured for half the scan time at the beginning and end of each scan. The stability of the crystal alignment was monitored by collecting two standard reflections every 23 measurements. A complete sphere of reflections (3026 measurements, exclusive of standards) was collected from 3 to 60° 2θ . Two of the reflections (0 0 3 and 0 0 $\bar{3}$) were rejected because of asymmetrical backgrounds. Eleven strong reflections uniformly distributed with regard to 2θ were measured at 5° intervals of Ψ (the azimuthal angle corresponding to rotation of the crystal about its diffraction vector) from 0 to 350°, after the method of North *et al.* (1968). These data (792 measurements) were used to calculate an absorption correction. The crystal was modeled as a thin plate parallel to (0 0 1). A minimum glancing angle of 4° resulted in the loss of 132 reflections. The merging R index for the Ψ -scan data set decreased from 6.3% before the absorption correction to 4.8% after the absorption correction. This correction was then applied to the entire dataset; minimum and maximum transmissions were 0.68 and 0.90, respectively. The data were also corrected for Lorentz, polarization, and background effects, averaged and reduced to structure factors. Seventeen reflections were rejected because of inconsistent equivalents; of the remaining 307 unique reflections, 272 were classed as observed [$F_o > 4\sigma(F_o)$].

Structure solution and refinement

The Siemens SHELX-97 (Sheldrick 1997) system of programs was used throughout this study. Miscellaneous information about data collection and refinement are given in Table 1.

Previous single-crystal X-ray studies of minerals in the alunite supergroup have shown that almost all crystallize in space group $R\bar{3}m$ (Jambor 1999). Hence, re-

TABLE 1. ARGENTOJAROSITE: DATA COLLECTION AND STRUCTURE-REFINEMENT INFORMATION

a (Å)	7.3398(7)	$F_o > 4\sigma F_o$	272
c (Å)	16.538(3)	R_{int}	0.06(3)
V (Å ³)	771.4(2)	L.s. parameters	29
Space Group	$R\bar{3}m$ (no. 166)	R_1 for $F_o > 4\sigma F_o$	0.0229
Z	3	R_2 for all unique F_o	0.0276
Crystal size (mm)	$0.10 \times 0.09 \times 0.007$	wR_2	0.0541
Radiation	MoK α	a	0.0267
Monochromator	graphite	b	1.89
Total F_o	2464	Goodness of fit (S)	1.102
Unique F_o	307		

Note: $w = 1/[\sigma^2(F_o^2) + (a \times P)^2 + b \times P]$ where $P = [\text{Max}(F_o^2, 0) + 2 \times F_o^2]/3$

TABLE 3. SELECTED INTERATOMIC DISTANCES (Å) AND ANGLES (°) FOR ARGENTOJAROSITE

A-O(1)a	× 6	2.963(2)	O(1)a-A-O(1)d	× 2	67.70(4)
-OHa	× 6	2.721(2)	-O(1)e	× 2	112.30(4)
<A-O>		2.842	-OHa	× 6	70.54(6)
			-OHf	× 6	109.46(6)
G-O(1)b	× 2	2.048(2)	-OHg	× 12	120.73(4)
-OHc	× 4	1.9905(9)	-OHh	× 12	59.27(4)
<G-O>		2.010	OHf-A-OHh	× 6	61.09(7)
			-OHe	× 6	118.91(7)
T-O(1)c	× 3	1.481(2)	<O-A-O>		90.00
-O(2)		1.464(4)			
<T-O>		1.477	O(1)c-G-OHi	× 4	91.50(7)
			-G-OHj	× 4	88.50(7)
OH-H		0.980(1)	OHc-G-OHi	× 2	88.0(1)
H-O(2)c		1.876(4)	-OHj	× 2	92.0(1)
OH-O(2)c		2.856(3)	<O-G-O>		90.0
			O(1)c-T-O(1)k	× 3	109.51(9)
			-O(2)	× 3	109.43(9)
			<O-T-O>		109.47
			OH-H-O(2)c		177(5)

Note: $\langle M-\phi \rangle$ denotes the mean metal-ligand distance (Å). Equivalent positions: a = $-x + \frac{1}{2}, -y + \frac{1}{2}, -z + \frac{1}{2}$; b = $y, -x + y, -z$; c = $-x + \frac{1}{2}, -y + \frac{1}{2}, -z + \frac{1}{2}$; d = $-x + y - \frac{1}{2}, -x + \frac{1}{2}, z + \frac{1}{2}$; e = $x - y + \frac{1}{2}, x - \frac{1}{2}, -z + \frac{1}{2}$; f = $x - \frac{1}{2}, y - \frac{1}{2}, z + \frac{1}{2}$; g = $y - \frac{1}{2}, -x + y - \frac{1}{2}, -z + \frac{1}{2}$; h = $-y + \frac{1}{2}, x - y + \frac{1}{2}, z + \frac{1}{2}$; i = $x - y + \frac{1}{2}, x - \frac{1}{2}, -z + \frac{1}{2}$; j = $-x + y + \frac{1}{2}, -x + \frac{1}{2}, z - \frac{1}{2}$; k = $x - y + \frac{1}{2}, x - \frac{1}{2}, -z + \frac{1}{2}$.

The $\text{Fe}^{3+}\text{O}_2(\text{OH})_4$ octahedra share corner OH atoms to form sheets perpendicular to the c axis (Fig. 2). The OH groups form a plane roughly parallel to (001). The O(1) atoms lie on opposite sides of the OH layers. The octahedra form six- and three-membered rings, and the three apical O(1) atoms from each triad of octahedra form the base of a SO_4 tetrahedron. Additional sheets of octahedra are located in such a way that two triads of OH ions enclose a site in which the 12-coordinated Ag^+ ion is located (Fig. 2). The apical O(2) atoms on each of the SO_4 tetrahedra point alternately up and down the c axis, and project into the six-membered rings of hy-

TABLE 4. BOND-VALENCE* ANALYSIS OF ARGENTOJAROSITE

Site	A (Ag^+)	G (Fe^{3+})	T (S^{6+})	H	Total
O(1)	0.04 × 6 ↓	0.46 × 2 ↓	1.47 × 3 ↓		1.97
O(2)			1.54	0.08 × 3 →	1.78
OH	0.08 × 6 ↓	0.53 × 4 ↓ × 2 →		0.92	2.06
Total	0.72	3.04	5.95	1.00	

*Calculated from the curves of Brese & O'Keeffe (1991).

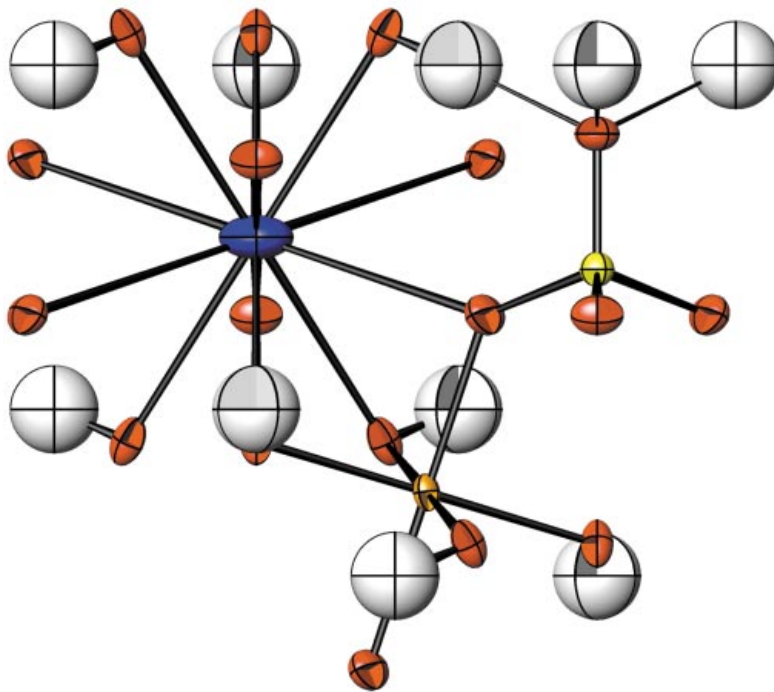


Fig. 1. Coordination polyhedra of cations in the argentojarosite structure, projected onto (100). The blue, orange, yellow, and red ellipsoids represent Ag, Fe, S, and O atoms, respectively. The atomic displacement ellipsoids represent 75% probability.

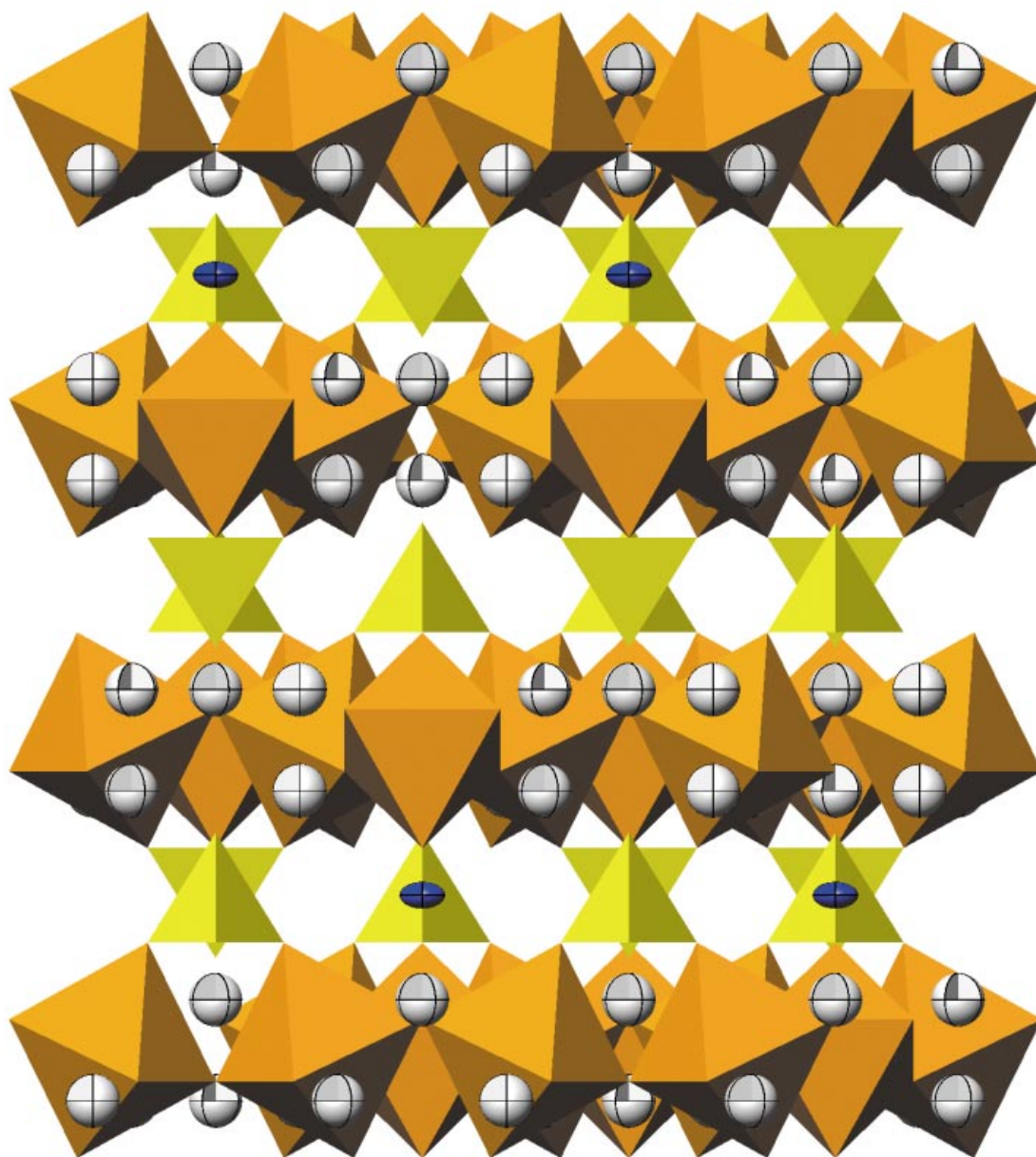


FIG. 2. The structure of argentojarosite projected onto (100), with c vertical, showing $\text{Fe}^{3+}\text{O}_2(\text{OH})_4$ octahedra, SO_4 tetrahedra, H atoms (grey spheres), and Ag atoms (blue ellipsoids). The atomic displacement ellipsoids represent 75% probability.

droxyl groups. Each O(2) atom forms weak hydrogen bonds with the three closest hydroxyl groups.

DISCUSSION

The members of the jarosite group of the alunite supergroup (Dutrizac & Jambor 2000), wherein the T

site is dominated by S^{6+} and the G position by Fe, are ammoniojarosite, argentojarosite, beaverite, dorallcharite, hydronium jarosite, jarosite, natrojarosite, and plumbojarosite. Stoffregen *et al.* (2000) showed that for minerals of the alunite supergroup, a is affected mainly by Al– Fe^{3+} substitutions, whereas variation in c largely reflects substitutions at the alkali site. Dutrizac &

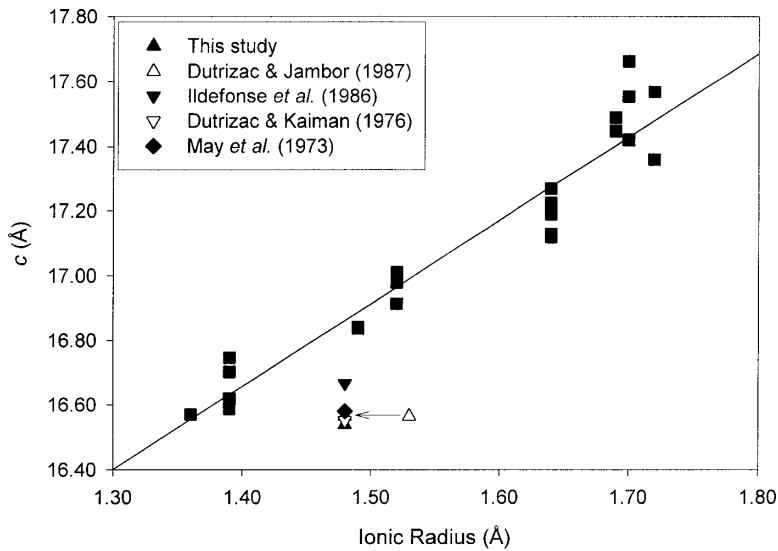


FIG. 3. Graph of c versus ionic radius (both in Å) for members of the jarosite subgroup (adapted from Dutrizac & Jambor 2000). The symbols in the box refer to argentojarosite data only. The equation for the regression line (based on non-argentojarosite data points) is $c = 2.568(\text{IR}) + 13.062$ ($R^2 = 0.92$).

Jambor (2000) plotted cell dimensions *versus* ionic radii for the members of the jarosite subgroup. As expected, they found considerable scatter in the plot for a , but a good correlation in the data for c . An exception pertains to the points for argentojarosite, which plot well below a regression line based on data for the other members of the subgroup (Fig. 3). This suggests an error in the ionic radius assumed for Ag^+ (1.48 Å), which was based on the ionic radius for 12-coordinated Pb (Dutrizac & Jambor 2000). Ignoring the value proposed by Ildefonse *et al.* (1986), which is for a sample with only 86 mol.% Ag, the regression equation returns radii for 12-coordinated Ag^+ of 1.35–1.37 Å. If the ionic radius of OH^- (1.32 Å; Shannon 1976) is subtracted from the A –OH bond distance, the result is a radius of 1.40 Å for Ag^+ , which is close to that derived from Figure 3.

In Figure 4, the ionic radii (from Shannon 1976) are plotted against coordination number for the A -site cations Ag, Tl, K, and Na. The regression equation returns a radius of 1.56 Å for 12-coordinated Ag^+ . Conversely, radii of 1.35–1.37 Å correspond to coordination numbers of 8.93–9.22; thus, the Ag^+ ion in argentojarosite has a radius more typical of nine-coordinated Ag^+ . The A –O(1) distances are very long, and the net effect is considered to be a coordination that is intermediate between six-fold and 12-fold, thereby resulting in a lower-than-expected ionic radius for Ag^+ . The underlying cause of this disagreement could be that the Ag^+ ion preferentially adopts small coordination numbers and favors short covalent bonds (Behrens *et al.* 1995).

In Table 2, we show that U_{eq} for the Ag atom is relatively high, and the U_{ij} values are somewhat anomalous. To U. Kolitsch (written commun., 2003), these anomalies could indicate that the Ag atom is located slightly off the site, with correspondingly reduced occupancy. The high value could indicate that the void is too big for Ag, and that the Ag ion tries to locally achieve lower coordination-numbers.

The low bond-valence sum to the A site (Table 4) deserves some comment. We point out that 12-coordinated Ag is not found in any other mineral species, and in very few synthetic compounds. Among the latter is AgBePO_4 (Hammond *et al.* 1998), in which the Ag(1) position is 12-coordinated, with Ag–O bond distances of 2.605–3.132 Å. The corresponding bond-valence sum is only 0.86 valence units. This value raises the strong possibility that the bond-valence curves (taken in this case from Brese & O’Keeffe 1991) cannot be applied to this coordination of Ag.

ACKNOWLEDGEMENTS

We thank M.A. Cooper for help with SHELX-97. The manuscript was improved by comments from V. Bermanec, U. Kolitsch and R.F. Martin. Financial support was provided by the Natural Sciences and Engineering Research Council of Canada in the form of a Research Grant to LAG, and by equipment grants from the BC Science and Technology Development Fund and the University of British Columbia.

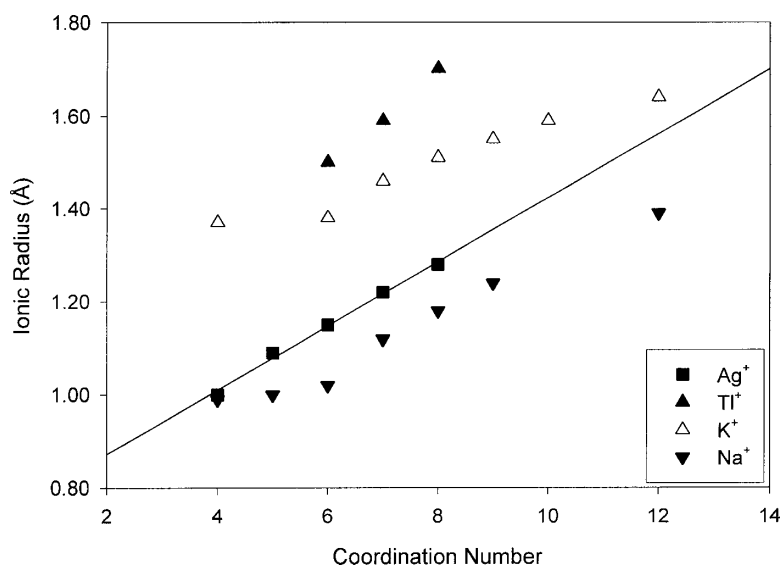


FIG. 4. Graph of ionic radius (in Å) versus coordination number (data from Shannon 1976). The equation for the regression line for Ag⁺ is ionic radius = 0.069(coordination number) + 0.734 ($R^2 = 0.99$).

REFERENCES

- AMORÓS, J.L., LUNAR, R. & TAVIRA, P. (1981): Jarosite: a silver bearing mineral of the gossan of Rio Tinto (Huelva) and la Unión (Cartagena, Spain). *Mineral. Deposita* **16**, 205-213.
- BARON, D. & PALMER, C.D. (1996): Solubility of $\text{KFe}_3(\text{CrO}_4)_2(\text{OH})_6$ at 4 to 35°C. *Geochim. Cosmochim. Acta* **60**, 3815-3824.
- BEHRENS, P., KEMPA, P.B., ASSMANN, S., WIEBCKE, M. & FELSCH, J. (1995): The structures of anhydrous silver sodalite $\text{Ag}_3[\text{Al}_3\text{Si}_3\text{O}_{12}]$ at 298, 623, and 723 K from Rietveld refinements of X-ray powder diffraction data: mechanism of thermal expansion and of the phase transition at 678 K. *J. Solid State Chem.* **115**, 55-65.
- BRESE, N.E. & O'KEEFFE, M. (1991): Bond-valence parameters for solids. *Acta Crystallogr.* **B47**, 192-197.
- DUTRIZAC, J.E. (1983): Factors affecting alkali jarosite precipitation. *Metall. Trans.* **14B**, 531-539.
- _____ & JAMBOR, J.L. (1985): Formation and characterization of argentojarosite and plumbojarosite and their relevance to metallurgical processing. In *Applied Mineralogy* (W.C. Park, D.M. Hausen & R.D. Hagni, eds.). Am. Inst. Mining Metall. Petroleum Eng., Warrendale, Pennsylvania (507-530).
- _____ & _____ (1987): Behaviour of silver during jarosite precipitation. *Trans. Inst. Mining Metall.* **C96**, 206-217.
- _____ & _____ (2000): Jarosites and their application in hydrometallurgy. In *Sulfate Minerals: Crystallography, Geochemistry, and Environmental Significance* (C.N. Alpers, J.L. Jambor & D.K. Nordstrom, eds.). *Rev. Mineral. Geochem.* **40**, 405-452.
- _____, _____ & O'REILLY, J.B. (1983): Man's first use of jarosite: the pre-Roman mining-metallurgical operations at Rio Tinto, Spain. *Can. Inst. Mining Metall., Bull.* **76**(859), 78-82.
- _____ & KAIMAN, S. (1976): Synthesis and properties of jarosite-type compounds. *Can. Mineral.* **14**, 151-158.
- GASHAROVA, B., GÖTTLICHER, J., BERNOTAT-WULF, H. & PENTINGHAUS, H. (2000): Single crystal structure refinement and Raman spectra of synthetic natrojarosite ($\text{NaFe}_3(\text{SO}_4)_2(\text{OH})_6$) and $\text{KFe}_3(\text{CrO}_4)_2(\text{OH})_6$. *Ber. Deutsch. Mineral. Ges.* **12**(1), 54 (abstr.).
- GELATO, L.M. & PARTHÉ, E. (1987): STRUCTURE TIDY – a computer program to standardize crystal structure data. *J. Appl. Crystallogr.* **20**, 139-143.
- GÖTTLICHER, J. & GASHAROVA, B. (1999): Can jarosites be monoclinic? *Ber. Deutsch. Mineral. Ges.* **11**(1), 86 (abstr.).
- _____, _____ & BERNOTAT-WULF, H. (2000): Pseudotrigonal jarosites $(\text{K}, \text{H}_3\text{O})\text{Fe}_3(\text{SO}_4)_2(\text{OH})_6$. *Geol. Soc. Am., Program Abstr.* **32**(7), A180.
- HAMMOND, R., BARBIER, J. & GALLARDO, C. (1998): Crystal structures and crystal chemistry of AgXPO_4 (X = Be, Zn). *J. Solid State Chem.* **141**, 177-185.

- HAWTHORNE, F.C., GROAT, L.A. & EBY, R.K. (1989): Antlerite, $\text{Cu}_3\text{SO}_4(\text{OH})_4$, a heteropolyhedral wallpaper structure. *Can. Mineral.* **27**, 205-209.
- _____, KRIVOVICHEV, S.V. & BURNS, P.C. (2000): The crystal chemistry of sulfate minerals. In *Sulfate Minerals: Crystallography, Geochemistry, and Environmental Significance* (C.N. Alpers, J.L. Jambor & D.K. Nordstrom, eds.). *Rev. Mineral. Geochem.* **40**, 1-112.
- ILDEFONSE, J.P., LE TOULLEC, C. & PERROTEL, V. (1986): About the synthetic lead-silver jarosite solid solution. In *Experimental Mineralogy and Geochemistry, Int. Symp. (Nancy)*, Abstr. Vol., 72-73.
- JAMBOR, J.L. (1999): Nomenclature of the alunite supergroup. *Can. Mineral.* **37**, 1323-1341.
- KOLITSCH, U. & PRING, A. (2001): Crystal chemistry of the crandallite, beudantite and alunite groups: a review and evaluation of the suitability as storage materials for toxic metals. *J. Mineral. Petrol. Sci.* **96**, 67-78.
- MAY, A., SJORBERG, J.J. & BAGLIN, E.G. (1973): Synthetic argentojarosite: physical properties and thermal behavior. *Am. Mineral.* **58**, 936-941.
- MENCHETTI, S. & SABELLI, C. (1976): Crystal chemistry of the alunite series: crystal structure refinement of alunite and synthetic jarosite. *Neues Jahrb. Mineral., Monatsh.*, 406-417.
- NEKRASOV, I.YA. & NIKISHOVA, L.V. (1987): First find of argentojarosite in the USSR. *Mineral. Zh.* **9**(1), 90-95 (in Russ.).
- NORTH, A.C.T., PHILLIPS, D.C. & MATHEWS, F.S. (1968): A semi-empirical method of absorption correction. *Acta Crystallogr.* **A24**, 351-359.
- PALACHE, C., BERMAN, H. & FRONDEL, C. (1951): *The System of Mineralogy* **2**. John Wiley & Sons, New York, N.Y.
- PEARL, R.M. (1974): Argentojarosite; new Colorado mineral. *Rocks & Minerals* **49**, 373.
- ROBINSON, K., GIBBS, G.V. & RIBBE, P.H. (1971): Quadratic elongation: a quantitative measure of distortion in coordination polyhedra. *Science* **172**, 567-570.
- ROCA, A., VIÑALS, J., ARRANZ, M. & CALERO, J. (1999): Characterization and alkaline decomposition/cyanidation of beudantite-jarosite materials from Rio Tinto gossan ores. *Can. Metall. Quart.* **38**, 93-103.
- SCHALLER, W.T. (1923): Argentojarosite, a new silver mineral. *J. Wash. Acad. Sci.* **13**, 233.
- SCHEMPF, C.A. (1923): Argento-jarosite, a new silver mineral. *Am. J. Sci.* **206**, 73-75.
- SHANNON, R.D. (1976): Revised effective ionic radii and systematic studies of interatomic distances in halides and chalcogenides. *Acta Crystallogr.* **A32**, 751-767.
- SHELDRIK, G.M. (1997): *SHELX-97. Program for the Refinement of Crystal Structures*. University of Göttingen, Göttingen, Germany.
- STOFFREGEN, R.E., ALPERS, C.N. & JAMBOR, J.L. (2000): Alunite-jarosite crystallography, thermodynamics, and geochronology. In *Sulfate Minerals: Crystallography, Geochemistry, and Environmental Significance* (C.N. Alpers, J.L. Jambor & D.K. Nordstrom, eds.). *Rev. Mineral. Geochem.* **40**, 453-479.
- SZYMAŃSKI, J.T. (1985): The crystal structure of plumbogjarosite $\text{Pb}[\text{Fe}_3(\text{SO}_4)_2(\text{OH})_6]_2$. *Can. Mineral.* **23**, 659-668.
- TROXEL, B.W. & MORTON, P.K. (1962): Mines and mineral resources of Kern County, California. *Calif. Div. Mines Geol., County Rep.* **1**.

Received July 14, 2002, revised manuscript accepted July 24, 2003.